ESRF	**Experiment title:** Electrocatalysts for PEM water electrolysis	**Experiment number:** 01-01-670
Beamline: BM01B	**Date of experiment:** from: 17.02.05 to: 22.02.05	**Date of report:** 14.03.2005 *Received at ESRF:*
Shifts: 18	**Local contact(s):** Wouter van Beek	

Names and affiliations of applicants (* indicates experimentalists):

*Aaron Marshall (1)
*Sten-Egil Johnsen (1)
*Mikhail Tsypkin (1)
*Nina Hammer (2)
*Magnus Rønning (2)
(1) Department of Materials Technology, NTNU
(2) Department of Chemical Engineering, NTNU
N-7491 Trondheim, Norway

Introduction:

Proton exchange membrane (PEM) water electrolysers have been shown to be a promising method of producing carbon free hydrogen [1]. Recently IrO_2 based materials have been examined as the anode or oxygen evolution electrode in our group [2-3]

In order to improve the properties of the electrocatalyst, in particular the activity towards oxygen evolution and stability, we have synthesised a range of materials based on iridium oxide. Additions of tin and titanium are shown to improve stability [4-6], whereas addition of ruthenium to the oxide structure improves the electrocatalytic activity. The electrocatalytic properties of the materials are strongly related to the structure of the oxides. In terms of stabilising the oxide structure we desire a solid solution between the active oxide (i.e. IrO_2 or RuO_2) and the stabilising oxide (e.g SnO_2). Solid state redox transitions are also very important in determining the activity of such materials [7].

X-ray diffraction studies have shown that the structure is highly dependent of the synthesis method, and we have been successful in producing both solid solution oxides and two phase oxides. As the most active materials are nanocrystalline or amorphous, precise structural analysis by diffraction techniques is not possible. This structure analysis will help explain the observed electrochemical properties of the materials.

In-situ electrochemical and structural analysis of the electrocatalysts will further advance the knowledge concerning how the structure influences the surface reactions. Previously it has been seen that the Ir-O [8] and Ru-O [9] bond lengths change with the applied potential (due to change in valence state). We want to extend the study to systems where there are two active elements (e.g. $Ir_xRu_{1-x}O_2$) and also non-active elements (e.g. $Ir_xSn_{1-x}O_2$) present in the lattice.

Experimental:

The powder samples were prepared in sealed sample holders and optimised for transmission XAFS measurements. These powder samples consisted of a range of compositions of the type $Ir_xSn_{1-x}O_2$ and $Ir_xRu_{1-x}O_2$. The XAFS measurements were performed on the powder samples at the Ir L_{III}-edge (11 212 eV) and when the samples contained ruthenium, at the Ru K-edge (22 119 eV) as well.

To study the oxide samples in-situ during electrochemical polarisation, a new in-situ Electrochemical / XAS cell was developed (Figure 1). In this cell the oxide samples were coated (around 0.5 mg/cm^2) onto graphite foil which acted as the electrical contact, catalyst support and X-ray window. This oxide-graphite composite was then used as the working electrode fro a series of electrochemical / XAS measurements. This was achieved by placing the oxide layer in contact with an aqueous 0.5 M H_2SO_4 electrolyte, parallel to a platinum counter electrode which completed the electrical circuit. A reversible hydrogen electrode (RHE) was also placed in the electrolyte, with the potential of the working electrode measured and controlled relative to this reference potential, using a Voltalab PZG 100 potentiostat from Radiometer Analytical. The XAS measurements were made by aligning the incoming x-ray beam to centre of the working electrode. The resulting fluorescence signal was then recorded using a 13 element solid state detector (Figure 2).

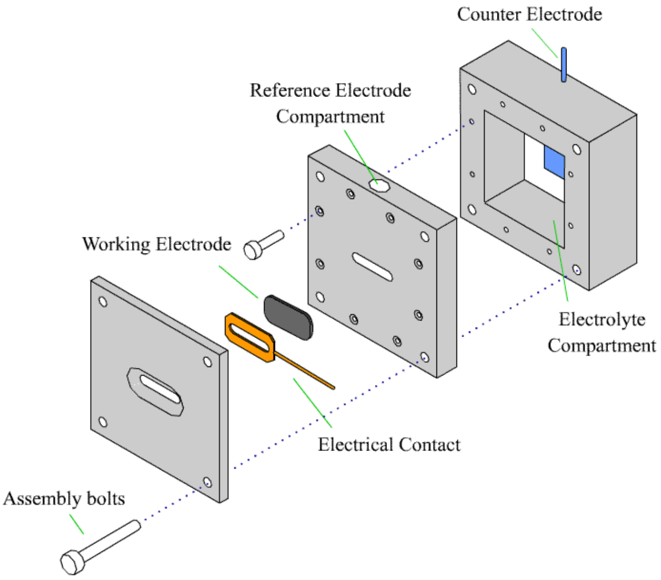

Figure 1. In-situ Electrochemical / X-ray Absorption Spectroscopy cell

Results:

EXAFS analysis of the $Ir_xSn_{1-x}O_2$ powders revealed that previous conclusions based on analysis using XRD may be incorrect. The Fourier transform of the EXAFS is shown in Figure 3, and reveals that the first iridium-metal shells do not change significantly with the bulk tin content and in fact correspond closely with the shells found in the IrO_2 standard, indicating that the oxide consists of primarily of IrO_6^{2-} octahedrons which surround the core iridium atom which is probed. This indicates that mixing at the atomic level of iridium and tin does not occur.

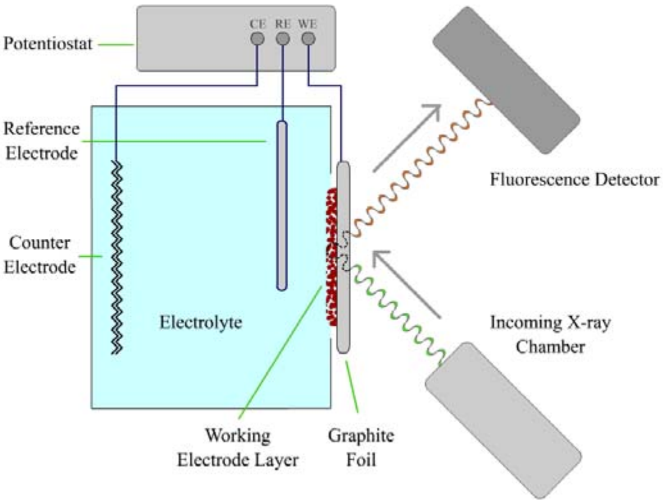

Figure 2. Principle of In-situ Electrochemical / X-ray Absorption Spectroscopy cell

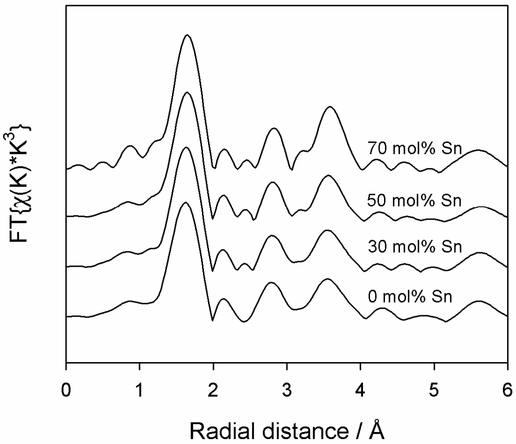

Figure 3. Fourier transform of the EXAFS from $Ir_xSn_{1-x}O_2$

The in-situ electrochemical / XAS measurements proved successful. Figure 4 shows the cell in use at BM01B. The majority of measurements show very good signal to noise ratio, indicating that this electrode arrangement can be used with no further developments in equipment. Initial results showed that as the electrode potential was made more positive, the white line energy increased by around 0.3 eV (Figure 5). This indicates to us that some change in the iridium valence has occurred. From the EXAFS analysis, we have also found that the iridium-oxygen bond length decreases in a linear fashion with increasing anodic potential (Figure 6). Further analysis of the XANES profile and EXAFS is ongoing.

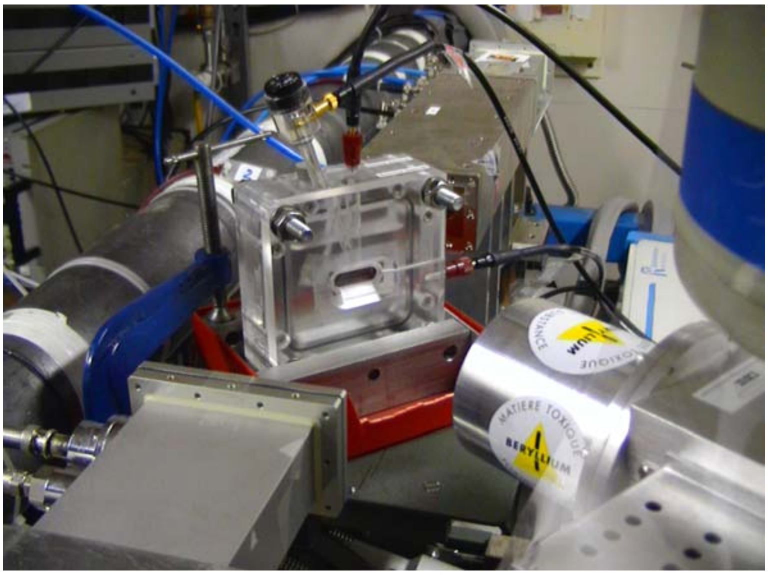

Figure 4 In-situ Electrochemical / X-ray Absorption Spectroscopy cell

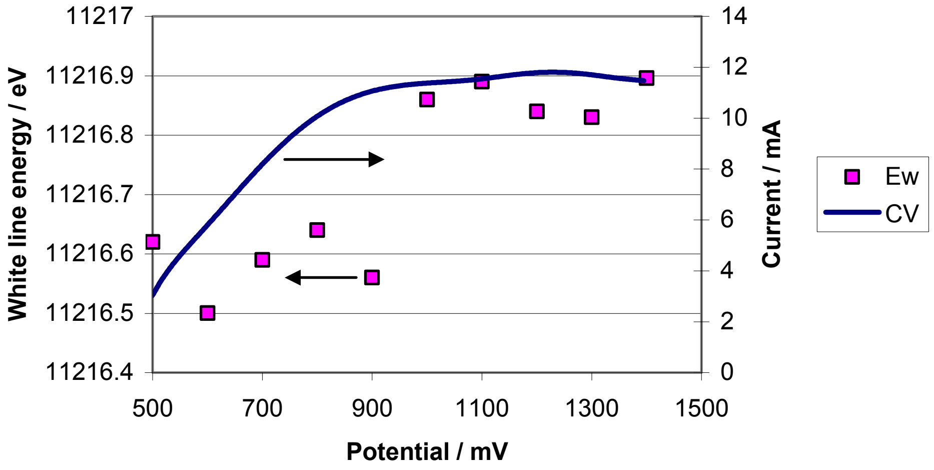

Figure 5. White line energy and voltammetric curve as a function of electrode potential. IrO_2 in 0.5 M H_2SO_4

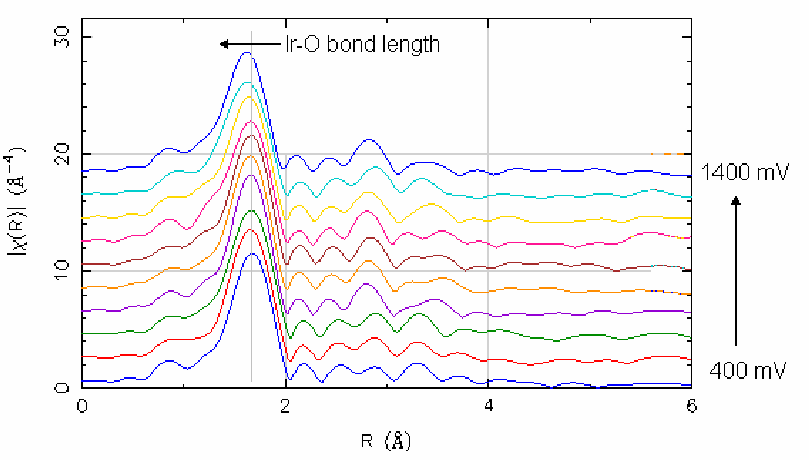

Figure 6. FT(EXAFS) of IrO_2 in 0.5 M H_2SO_4 as a function of electrode potential.

References:

[1] Oberlin R. Fischer M. *Hydrogen Energy Progress VI, Proceedings of the 6th World Hydrogen Energy Conference* 1 (1986) 333-340.

[2] Rasten E. Hagen G. Tunold R. *Proceedings - Electrochemical Society* 23 (2001) 151-164.

[3] Rasten E. Hagen G. Tunold R. *Electrochim. Acta* 48 (2003) 3945-3952.

[4] Hutchings R. Müller K. Stucki S. *J. Ma. Sci.* 19 (1984) 3987-3994.

[5] De Pauli C. and Trasatti S. *J. Electroanal. Chem.* 396 (1995) 161-168

[6] Endo K. Katayama Y. Miura T. Kishi T. *J. Applied Electrochem.* 32 (2002) 173-178. Mo Y. Stefan I. Cai W. Dong J. Carey P. Scherson D. *J. Phys. Chem. B* 106 (2002) 3681-3686.

[7] Trasatti S. *The oxygen evolution reaction, Electrochemical Hydrogen Technologies* (1990) 104-135

[8] Mo Y. Stefan I. Cai W. Dong J. Carey P. Scherson D. *J. Phys. Chem. B* 106 (2002) 3681-3686.

[9] Mo Y. Antonio M. Scherson D. *J. Phys. Chem. B* 104 (2000) 9777-9779.